

Universality aspects of the 2d random-bond Ising and 3d Blume-Capel models

N.G. Fytas^{1a} and P.E. Theodorakis^{2,3}

¹ Departamento de Física Teórica I, Universidad Complutense, E-28040 Madrid, Spain

² Faculty of Physics, University of Vienna, Boltzmanngasse 5, 1090 Vienna, Austria

³ Institute for Theoretical Physics and Center for Computational Materials Science, Vienna University of Technology, Hauptstraße 8-10, 1040 Vienna, Austria

Received: date / Revised version: date

Abstract. We report on large-scale Wang-Landau Monte Carlo simulations of the critical behavior of two spin models in two- (2d) and three-dimensions (3d), namely the 2d random-bond Ising model and the pure 3d Blume-Capel model at zero crystal-field coupling. The numerical data we obtain and the relevant finite-size scaling analysis provide clear answers regarding the universality aspects of both models. In particular, for the random-bond case of the 2d Ising model the theoretically predicted strong universality's hypothesis is verified, whereas for the second-order regime of the Blume-Capel model, the expected $d = 3$ Ising universality is verified. Our study is facilitated by the combined use of the Wang-Landau algorithm and the critical energy subspace scheme, indicating that the proposed scheme is able to provide accurate results on the critical behavior of complex spin systems.

PACS. PACS. 05.50+q Lattice theory and statistics (Ising, Potts. etc.) – 64.60.De Statistical mechanics of model systems

1 Introduction

Universality, according to which the same critical exponents occur in all second-order phase transitions between the same two phases, erstwhile phenomenologically established, has been a leading principle of critical phenomena [1]. The explanation of universality, in terms of diverse Hamiltonian flows to a single fixed point, has been one of the crowning achievements of renormalization-group theory [2]. In rather specialized models in spatial dimension $d = 2$, such as the eight-vertex [3] and Ashkin-Teller [4] models, the critical exponents nevertheless vary continuously along a line of second-order transitions, a phenomenon referred to as the weak violation of universality. Although the existence and quantitative description of universality classes in most pure spin systems with simple interactions is well-established, this is not true for more realistic models that include competing interactions and/or disorder [5, 6].

In the current manuscript we discuss the universality aspects of two distinct complex, in terms of randomness and interactions, spin models, yielding exact information on their critical behavior by applying finite-size scaling (FSS) techniques to high-accuracy numerical data. In particular, we investigate the 2d Ising model under the presence of quenched uncorrelated bond randomness and a

generalized 3-spin state Ising model with an additional crystal-field coupling interaction in $d = 3$, known as the Blume-Capel model [7, 8], for a certain regime of its phase diagram. For the first 2d (random) model, for which its exact phase diagram is known, we present comparative results for two distinct values of the disorder strength and we give concrete evidence in favor of the theoretically proposed strong universality hypothesis [9–13]. For the latter 3d (pure) Blume-Capel model, which we choose to simulate in the regime of its phase diagram where Ising-like continuous transitions are known to take place [7, 8], we consider a particular value of the crystal field and present high-accuracy results for very large lattice sizes that indeed place the model in the universality class of the respective 3d Ising model.

Our study benefits from the Wang-Landau (WL) algorithm [14], including some recently proposed variations, namely the critical minimum energy subspace technique of Malakis et al. [15] on the reduction of the energy spectrum of the simulation, and the proposal of Belardinelli and Pereyra [16] regarding the application of the energy-histogram flatness criterion of the original WL method. The details of this implementation, as well as the general framework of the WL approach are given in the next Section. Subsequently, in Section 3 we discuss the universality aspects of the models, providing also estimates of their critical exponents, which are found to be in good

^a e-mail: nfytas@phys.uoa.gr

agreement with relevant existing estimates in the literature. This paper is ended in Section 4 with a summary of our conclusions.

2 Simulation method

Importance sampling methods have been for many years the main tools in condensed matter physics and critical phenomena [17–21]. However, for complex systems, effective potentials may have a rugged landscape, that becomes more pronounced with increasing system size. In such cases, these traditional methods become inefficient, since they cannot overcome large barriers in the state space. A vast number of generalized ensemble methods have been proposed to overcome this type of problems [14, 20–35]. One important class of these methods emphasizes the idea of directly sampling the energy density of states (DOS) and may be called entropic sampling methods [20]. In entropic sampling, instead of sampling microstates with probability proportional to $e^{-\beta E}$, one samples microstates with probability proportional to $[G(E)]^{-1}$, where $G(E)$ is the DOS, thus producing a flat energy histogram. The prerequisite for the implementation of the method is the DOS information of the system, a problem that can now be handled in many adequate ways via a number of interesting approaches proposed in the last two decades. The most remarkable examples are the Lee entropic [22, 23], the multicanonical [26, 27], the broad histogram [24], the transition matrix [25], the WL [14], and the optimal ensemble methods [35]. In particular, there is a considerable interest in the WL method and this is manifested in the growing number of relevant publications that stem from nearly every branch of the community of statistical mechanics. The WL method is becoming a standard tool in examining simple, but also more rugged, free-energy landscapes, in both magnetic and soft matter systems and several papers dealing with improvements and sophisticated implementations of its iterative process have appeared throughout the years [15, 16, 36–63].

To apply the WL algorithm, an appropriate energy range of interest has to be identified and a WL random walk is performed in this energy subspace. Trials from a state with energy E_i to a spin state with energy E_f are accepted according to the transition probability

$$p(E_i \rightarrow E_f) = \min \left[\frac{G(E_i)}{G(E_f)}, 1 \right]. \quad (1)$$

During the WL process the DOS $G(E)$ is modified $[G(E) \rightarrow fG(E)]$ after each trial by a modification factor $f > 1$. In the WL process ($j = 1, 2, \dots, j_{\text{final}}$) successive refinements of the DOS are achieved by decreasing the modification factor f_j . Most implementations use an initial modification factor $f_{j=1} = e \approx 2.71828 \dots$, a rule $f_{j+1} = \sqrt{f_j}$, and a 5% – 10% flatness criterion (on the energy histogram) in order to move to the next refinement level ($j \rightarrow j + 1$) [14]. The process is terminated in a sufficiently high-level ($f \approx 1$, whereas the detailed balanced condition limit is $f \rightarrow 1$).

In the last few years we have used an entropic sampling implementation of the WL algorithm [14] to study some simple [15], but also some more complex systems [53]. One basic ingredient of this implementation is a suitable restriction of the energy subspace for the implementation of the WL algorithm. This was originally termed as the critical minimum energy subspace restriction [15] and it can be carried out in many alternative ways, the simplest being that of observing the finite-size behavior of the tails of the energy probability density function of the system [15]. Assume that \tilde{E} denotes the value of energy producing the maximum term in the partition function of the statistical model, at some temperature of interest. Since we deal with a finite system of linear size L , we are interested in the properties (finite-size anomalies) near some pseudocritical temperature T_L^* , which in general depend on L but also on the property studied. Thus, we define a set of approximations by restricting the statistical sums to energy subranges around the value $\tilde{E} = \tilde{E}(T_L^*)$. Let these subranges of the total energy range (E_{\min}, E_{\max}) be denoted as

$$(\tilde{E}_-, \tilde{E}_+), \quad \tilde{E}_{\pm} = \tilde{E} \pm \Delta^{\pm}, \quad \Delta^{\pm} \geq 0. \quad (2)$$

Accordingly

$$\tilde{\Phi}(E) = [S(E) - \beta E] - \left[S(\tilde{E}) - \beta \tilde{E} \right], \quad \tilde{Z} = \sum_{\tilde{E}_-}^{\tilde{E}_+} \exp[\tilde{\Phi}(E)]. \quad (3)$$

Since by definition $\tilde{\Phi}(E)$ is negative we can easily see that for large lattices extreme values of energy (far from \tilde{E}) will have an extremely small contribution to the statistical sums, since these terms decrease exponentially fast with the distance from \tilde{E} . It follows that, if we request a specified accuracy, then we may restrict the necessary energy range in which DOS should be sampled. A simple idea is to use a condition based on the energy probability density ($f_{T_L^*}(E) \propto \tilde{\Phi}(E)$), meaning the application of Eq. (4) at a particular pseudocritical temperature T_L^* . That is, we may define the end-points (\tilde{E}_{\pm}) of the subspaces by simply comparing the corresponding probability densities with the maximum at the energy \tilde{E} :

$$\tilde{E}_{\pm} : \exp\{\tilde{\Phi}(\tilde{E}_{\pm})\} \leq r, \quad (4)$$

where r measures the relative error and it is usually set equal to a small number ($r = 10^{-6}$) [15]. This procedure ends by providing us with a restricted energy subrange (E_1, E_2) centered around the value \tilde{E} , where the large part of the simulation is finally carried out. Note that, in general, the location of these subspaces can be predicted either by extrapolation, from smaller lattices, or by using the early-stage DOS approximation of the WL method.

Complications that may arise in random systems can be easily accounted for by various simple modifications that take into account possible oscillations in the energy probability density function and expected sample-to-sample fluctuations of individual disorder realizations. In our recent papers [53], we have presented details of various sophisticated routes for the identification of the appropriate energy subspace (E_1, E_2) for the entropic sampling

of each random realization. In estimating the appropriate subspace from a chosen pseudocritical temperature one should be careful to account for the shift behavior of other important pseudocritical temperatures and extend the subspace appropriately from both low- and high-energy sides in order to achieve an accurate estimation of all finite-size anomalies. Of course, taking the union of the corresponding subspaces, insures accuracy for the temperature region of all studied pseudocritical temperatures.

The up to date version of our implementation uses a combination of several stages of the WL process. First, we carry out a starting (or preliminary) multi-range (multi-R) stage, in a very wide energy subspace. This preliminary stage may consist of the levels: $j = 1, \dots, 18$ of the adjustment of the modification factor and to improve accuracy the process may be repeated several times. However, in repeating the preliminary process and in order to be efficient, we use only the levels $j = 13, \dots, 18$ after the first attempt, using as starting DOS the one obtained in the first random walk at the level $j = 12$. From our experience, this practice is almost equivalent of simulating the same number of independent WL random walks. Also in our recent studies we have found out that is much more efficient and accurate to loosen up the originally applied very strict flatness criteria [14, 15]. Thus, a variable flatness process starting at the first levels with a very loose flatness criteria and assuming at the level $j = 18$ the original strict flatness criteria is nowadays used. After the above described preliminary multi-R stage, in the wide energy subspace, one can proceed in a safe identification of the appropriate energy subspace using one or more alternatives outlined in Ref. [15]. In random systems, where one needs to simulate many disorder realizations, it is also possible and advisable to avoid the identification of the appropriate energy subspace separately for each disorder realization by extrapolating from smaller lattices and/or by prediction from preliminary runs on small numbers of disorder realizations. In any case, the appropriate subspaces should be defined with sufficient tolerances. In our implementation we use such advance information to proceed in the next stages of the entropic sampling.

The process continues in two further stages (two-stage process), using now mainly high iteration levels, where the modification factor is very close to unity and there is not any significant violation of the detailed balance condition during the WL process. These two stages are suitable for the accumulation of energy and magnetization (E, M) histograms, which can be used for an accurate entropic calculation of non-thermal thermodynamic parameters, such as the order parameter M and its susceptibility χ [15]. In particular, the resulting approximation of the DOS and the corresponding E, M histograms may be used to estimate the magnetic properties of the system in a temperature range, which is covered, by the restricted energy subspace (E_1, E_2) . Canonical averages of the form

$$\langle M^n \rangle = \frac{\sum_E \langle M^n \rangle_E G(E) e^{-\beta E}}{\sum_E G(E) e^{-\beta E}}, \quad (5)$$

where $G(E)$ denotes the exact DOS, will be then approximated via

$$\langle M^n \rangle \cong \frac{\sum_{E \in (E_1, E_2)} \langle M^n \rangle_{E, \text{WL}} G_{\text{WL}}(E) e^{-\beta E}}{\sum_{E \in (E_1, E_2)} G_{\text{WL}}(E) e^{-\beta E}}, \quad (6)$$

with $G_{\text{WL}}(E)$ the DOS of the above described WL process. Then, the microcanonical averages $\langle M^n \rangle_E$ are obtained from the $H_{\text{WL}}(E, M)$ histograms through the following formulae

$$\langle M^n \rangle_E \cong \langle M^n \rangle_{E, \text{WL}} \equiv \sum_M M^n \frac{H_{\text{WL}}(E, M)}{H_{\text{WL}}(E)}. \quad (7)$$

As usual $H_{\text{WL}}(E) = \sum_M H_{\text{WL}}(E, M)$ and the summation in M runs over all values generated during the process in the restricted energy subspace (E_1, E_2) . The accuracy of the magnetic properties obtained from the above averaging process will depend on many factors. Firstly, the used energy subspace restricts the temperature range for which such approximations may be accurate. This restriction has as a result that the process will not visit all possible values of M , but this fact is of no consequence for the accuracy of the magnetic properties at the temperature range of interest, as far as the estimated DOS is accurate. Secondly, the accuracy of the above microcanonical estimators will, as usually, depend on the total number of visits to a given energy level $[H_{\text{WL}}(E)]$, and also to the number of different spin states visited within this energy level. However, these are statistical fluctuations inherent in any Monte Carlo method and we should expect improvement by increasing the number of repetitions of the process.

In the first (high-level) stage, we follow again a repeated several times (typically $\sim 5 - 10$) multi-R WL approach, carried out now only in the restricted energy subspace. The WL levels may be now chosen as $j = 18, 19, 20$ and as an appropriate starting DOS for the corresponding starting level the average DOS of the preliminary stage at the starting level may be used. Finally, the second (high-level) stage is applied in the refinement WL levels $j = j_i, \dots, j_i + 4$ (typically $j_i = 21$), where we usually test both an one-range (one-R) or a multi-R approach with large energy intervals. We should note here however that, most authors use the more efficient multi-R approach in the final stages of the WL process, as a consequence of the well-known slow convergence of the method at the high iteration-levels. We point out here that, it is possible to overcome this slow convergence by using a looser flatness criterion or an alternative Lee entropic final stage, as proposed in Ref. [23] and applied in Ref. [53]. Moreover, recently a different alternative has been proposed by Belardinelli and Pereyra (denoted hereafter as the BP approach) [16]. Following their proposal, one is using, in the final stage, an almost continuously changing modification factor adjusted according to the rule $\ln f \sim t^{-1}$. Since t is the Monte Carlo time, using a time-step conveniently defined proportional to the size of the energy subinterval, the efficiency of this scheme is independent of the size of the subintervals and therefore the method provides the same efficiency in both multi-R and one-R approaches.

Furthermore, from the tests performed by these authors, and also from our comparative studies in the 2d pure and random-bond Ising model, as will be seen below in Section 3, the error-behavior of this method seems superior to the original WL process, improving to some extent the saturation-error problem of the WL method and giving slightly better estimates of critical temperatures and exponents. Accordingly, we have also applied this alternative route for the final stage of our simulations using an one-R approach.

The above described numerical approach was used to estimate the critical properties of the considered spin models. In particular, for the random-bond version of the 2d Ising model we have simulated a very large number of disorder realizations (of the order of 500 – 1000, disorder averaging is symbolized as usual with $[\dots]_{\text{av}}$) for both values of the disorder strength considered and for systems with linear sizes in the range $L = 20 - 200$. For each lattice size we have performed two types of simulations: the original multi-R WL approach and the WL approach modified by the recent BP proposal [16]. In both cases the exact same disorder realizations have been generated and simulated, in order to have a direct comparison of the extracted critical behavior. Finally, for the pure version of the 3d Blume-Capel model at $\Delta = 0$, we simulated, using only the BP procedure in the final stage of our combined algorithm, simple cubic lattices with $N = L^3$ spins, where $L = 8 - 64$. For this case, each lattice size was simulated 100 times with different initial random numbers to get a better statistical analysis of the results.

Before closing, let us comment on the nature of our error bars illustrated in the following figures below and also used in the corresponding fitting attempts. For the case of the random-bond model, even for the larger lattice sizes studied, the statistical errors of the WL method were found to be of reasonable magnitude and in some cases to be of the order of the symbol sizes, or even smaller. Thus in the figures below we choose to show only the errors due to the finite number of disorder realizations. These errors have been estimated by two similar methods, using groups of 25 to 50 realizations for each lattice size and the jackknife method or a straightforward variance calculation (blocking method) [20]. The jackknife method yielded some reasonably conservative errors, about 10–20% larger than the corresponding calculated standard deviations, and are shown as error bars in our figures. Finally, let us point out that in all cases studied, the sample-to-sample fluctuations for the individual maxima are much larger than the corresponding finite disorder sampling errors. Finally, for the case of the pure Blume-Capel model, the error bars shown reflect the sample variance of the 100 independent runs performed in each lattice size.

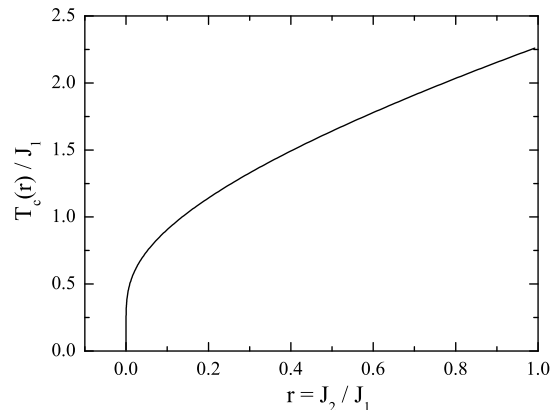


Fig. 1. Critical temperatures as a function of the disorder strength r of the 2d random-bond Ising model defined in Eqs. (8) and (9) obtained by solving Eq. (10).

3 Results and discussion

3.1 Strong universality in the 2d random-bond Ising model

Understanding the role played by impurities on the nature of phase transitions is of great importance, both from experimental and theoretical perspectives. First-order phase transitions are known to be dramatically softened under the presence of quenched randomness [64–73], while continuous transitions may have their exponents altered under random fields or random bonds [74, 75]. There are some very useful phenomenological arguments and some, perturbative in nature, theoretical results, pertaining to the occurrence and nature of phase transitions under the presence of quenched randomness [65, 68, 76, 77]. Historically, the most celebrated criterion is that suggested by Harris [74]. This criterion relates directly the persistence, under random bonds, of the non random behavior to the specific heat exponent α_p of the pure system. According to this criterion, if $\alpha_p > 0$, then disorder will be relevant, i.e., under the effect of the disorder, the system will reach a new critical behavior. Otherwise, if $\alpha_p < 0$, disorder is irrelevant and the critical behavior will not change.

Pure systems with a zero specific heat exponent are marginal cases of the Harris criterion and their study, upon the introduction of disorder, has been of particular interest [78]. The paradigmatic model of the marginal case is the general random 2d Ising model (random-site, random-bond, and bond-diluted) and this model has been extensively investigated and debated [see Refs. [79, 80] and references therein]. Several recent studies, both analytical (renormalization group and conformal field theories) and numerical (mainly Monte Carlo simulations) devoted to this model, have provided very strong evidence in favor of the so-called logarithmic corrections’s scenario [9–13, 81]. According to this, the effect of infinitesimal disorder gives rise to a marginal irrelevance of randomness and besides logarithmic corrections, the critical exponents maintain

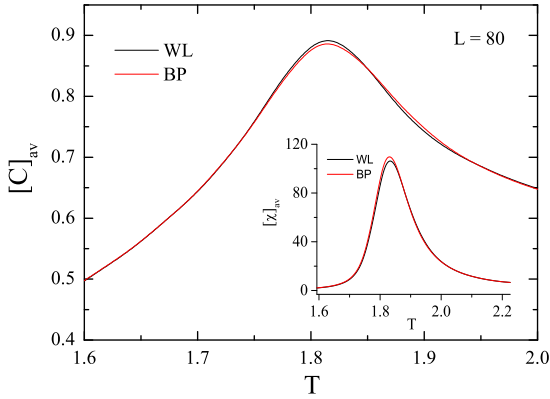


Fig. 2. (color online) A comparative plot of the disorder-averaged specific heat (main panel) and magnetic susceptibility (inset) as a function of temperature for a lattice size $L = 80$ and disorder strength $r = r_1 = 1/7$ of the 2d random-bond Ising model.

their 2d Ising values. Here, we should mention that there is not full agreement in the literature and a different scenario, the so-called weak universality scenario [82–85], predicts that critical quantities, such as correlation length display power-law singularities, with the corresponding exponents ν changing continuously with the disorder strength; however this variation is such that the magnetic exponent ratios remain constant at the pure system's value.

Here we present concrete evidence in favor of the strong universality scenario together with a comparative algorithmic test of the WL-type of methods presented above. Let us at this point define the quenched version of the 2d Ising model that we employ. In particular we choose to study here the random-bond version of the square lattice Ising model (RBIM), which is defined with the help of the following Hamiltonian

$$\mathcal{H}^{(\text{RBIM})} = - \sum_{\langle ij \rangle} J_{ij} s_i s_j. \quad (8)$$

In the above Eq. (8) the spin variables s_i take on the values $-1, +1$, $\langle ij \rangle$ indicates summation over all nearest-neighbor pairs of sites, and J_{ij} is the ferromagnetic exchange interaction taken from a bimodal, quenched bond-disorder, distribution of the form

$$\mathcal{P}(J_{ij}) = \frac{1}{2} [\delta(J_{ij} - J_1) + \delta(J_{ij} - J_2)], \quad (9)$$

where $J_1 + J_2 = 2$, $J_1 > J_2 > 0$, and $r = J_2/J_1$ reflects the strength of the bond randomness. We also fix $2k_B/(J_1 + J_2) = 1$ to set the temperature scale. With the above distribution the 2d random model exhibits a unique advantage, that is its critical temperature T_c is exactly known [86] as a function of the disorder strength r through the relation

$$\sinh(2J_1/T_c) \cdot \sinh(2rJ_1/T_c) = 1. \quad (10)$$

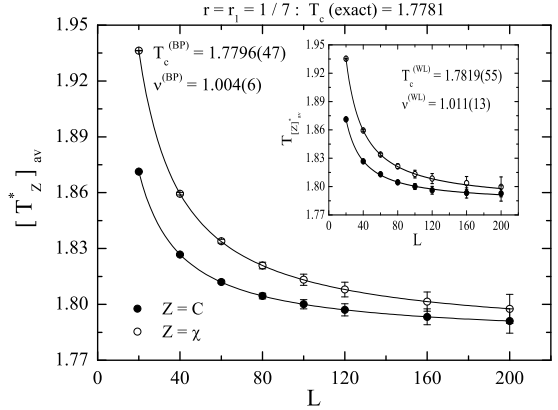


Fig. 3. Shift behavior of the pseudocritical temperatures of the specific heat and susceptibility, averaged over disorder, for the 2d random-bond Ising model with disorder strength $r = r_1 = 1/7$. The solid lines show a simultaneous fitting according to the power law described in the text for the total lattice range $L = 20 - 200$. The main panel shows the data and results obtained via the BP approach, whereas the inset via the WL approach.

The solution of the above Eq. (10), i.e. the function $T_c(r)$, is plotted in Fig. 1 and consists the phase diagram of the model in the temperature - disorder strength plane.

This unique feature of knowing exactly the critical temperature of a disordered model gives us the opportunity to perform a comparative FSS analysis of several pseudocritical temperatures for extracting estimates of the critical temperatures and shift exponents using the algorithmic procedures described above. In our simulations we have considered two values of the disorder strength, namely the values $r = r_1 = 1/7$ and $r = r_2 = 1/9$, both belonging to the strong-disorder regime of the model. The exact critical temperatures for these values of r are $T_c(r = r_1) = 1.7781 \dots$ and $T_c(r = r_2) = 1.6853 \dots$, respectively.

Our results for the 2d random-bond Ising model are shown in Figs. 2 - 4. We start with Fig. 2 which is a comparative illustration of the disorder-averaged specific heat $[C]_{\text{av}}$ and susceptibility $[\chi]_{\text{av}}$ curves as a function of temperature, estimated via the two approaches, WL and BP, used in this study. One may observe some small differences in the location (and the corresponding maximum value) of the peak in both specific heat and susceptibility data via the two implemented approaches. Subsequently, in Figs. 3 and 4 we plot the shift behavior of the disorder averaged pseudocritical temperatures of the specific heat and magnetic susceptibility as a function of the lattice size L and in all cases the solid lines illustrate a simultaneous fitting procedure of the form $[T_Z^*]_{\text{av}} = T_c + b_Z L^{-1/\nu}$, where $Z = C$ or $Z = \chi$, as shown by the corresponding symbols (filled and open circles) in the figures. In the main panels we present our numerical data obtained by applying in the final stage of the algorithmic procedure the BP approach (thus denoted by the superscript (BP)

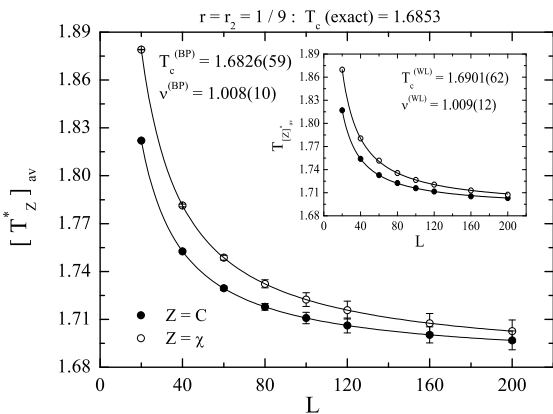


Fig. 4. Similar to Fig. 3 but for a different value of the disorder strength, namely $r = r_2 = 1/9$.

in the figures), whereas in the corresponding insets those of the original multi-R WL process (thus denoted by the superscript (WL) in the figures).

It is clear from both figures that the results obtained for the critical temperatures and also for the critical exponent of the correlation length are in excellent agreement with the exact values and also support the strong universality scenario hypothesis, via the relation $\nu = 1$. Also, they compare well to the results given by the extensive Swendsen-Wang Monte Carlo analysis of Wang et al. [81]. Finally, let us comment here that, although the computational time used for the BP approach is somewhat larger (of the order of ~ 2.5) than that of the simple multi-R WL process, the estimates obtained via this approach are slightly better than those of the simple multi-R WL procedure and this is true for both values of the disorder strength considered in this paper. Furthermore, other relevant tests performed originally in the simple case of the pure 2d Ising model and our experience of simulating rough random systems, such as the random-field Ising model [53] or systems undergoing first-order phase transitions in their pure versions [87], support the above illustration.

3.2 Ising universality in the Blume-Capel model

We investigate the universality of the 3d Blume-Capel in the second-order phase-transition regime of its phase diagram (temperature - crystal field plane) using the algorithmic procedure that combines a repetitive application of the WL algorithm in the first stage and the BP approach in the final stage of the algorithm. For this purpose, the static critical exponents are estimated by analyzing the obtained numerical data within the framework of the well-established FSS theory. At the same time, their values are calculated using power-law relations of related thermodynamic quantities. As also stated below, the 3d Blume-Capel model is expected to be in the universality class of the 3d Ising model for the second-order phase-

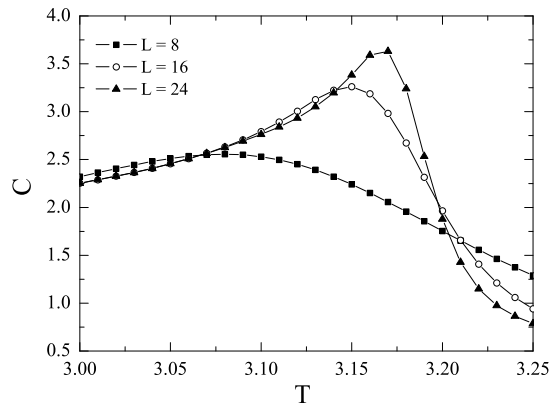


Fig. 5. Specific heat curves of the 3d $\Delta = 0$ Blume-Capel model as a function of temperature for $L = 8, 16$, and $L = 24$.

transition regime of its phase diagram. Thus, it is crucial at this point to remind the reader some of the best well-known estimates in the literature for the critical exponents of the 3d Ising model, as given in Ref. [88]: $\nu = 0.6304(13)$, $\gamma/\nu = 1.966(3)$, and $\beta/\nu = 0.517(3)$. For the most accurate complete set of critical exponents to the 3d Ising universality class we refer the reader to the review by of Pelissetto and Vicari [89].

Let us define at this point the Hamiltonian of the Blume-Capel (BC) model [7, 8]

$$\mathcal{H}^{(BC)} = -J \sum_{\langle ij \rangle} s_i s_j + \Delta \sum_i s_i^2, \quad (11)$$

where the spin variables s_i take on the values $-1, 0$, or $+1$, as usual $\langle ij \rangle$ indicates summation over all nearest-neighbor pairs of sites, and $J > 0$ is the ferromagnetic exchange interaction. The parameter Δ is known as the crystal-field coupling and to fix the temperature scale we set $J = 1$ and $k_B = 1$. This model is of great importance for the theory of phase transitions and critical phenomena and besides the original mean-field theory [7, 8], has been analyzed by a variety of approximations and numerical approaches, in both 2d and 3d. These include the real space renormalization group, Monte Carlo simulations, and Monte Carlo renormalization-group calculations [90], ϵ -expansion renormalization groups [91], high- and low-temperature series calculations [92], a phenomenological FSS analysis using a strip geometry [93, 94], and Monte Carlo simulations [87, 95–102]. The phase diagram of the model consists of a segment of continuous Ising-like transitions at high temperatures and low values of the crystal field which ends at a tricritical point, where it is joined with a second segment of first-order transitions between (Δ_t, T_t) and $(\Delta_0, T = 0)$. For the simple cubic lattice, considered in this paper, $\Delta_0 = 3$. The location of the tricritical point has been estimated by Deserno [98], via a microcanonical Monte Carlo approach, and is given by $[\Delta_t, T_t] = [2.84479(30), 1.4182(55)]$.

In what follows we restrict our analysis to the value $\Delta = 0$ and we simulate the Blume-Capel model for a wide

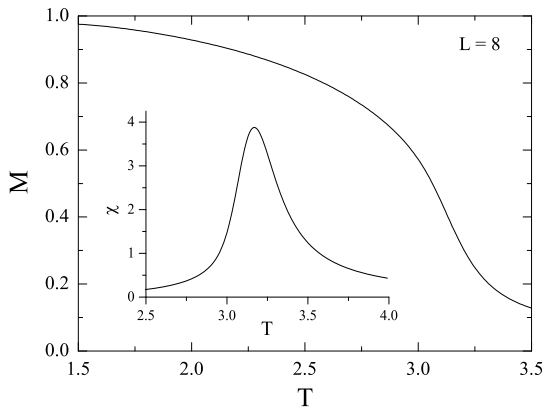


Fig. 6. Order-parameter (main panel) and corresponding magnetic susceptibility (inset) of the 3d $\Delta = 0$ Blume-Capel model as a function of the temperature for a lattice with linear size $L = 8$.

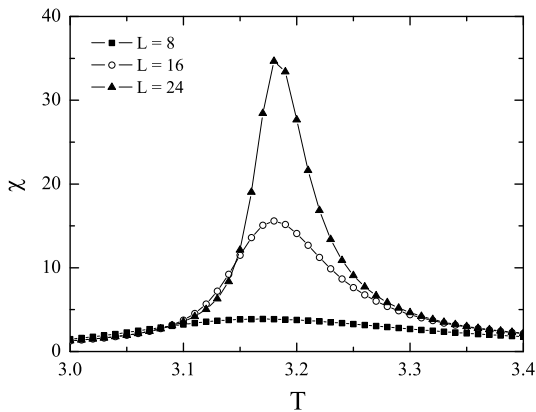


Fig. 7. Magnetic susceptibility curves of the 3d $\Delta = 0$ Blume-Capel model as a function of temperature for $L = 8, 16,$ and $L = 24$.

range of lattices, with linear sizes $L \in \{8, 16, 24, 32, 48, 64\}$, summing for each lattice size 100 independent simulations with different initial conditions in order to gain better statistics. Moreover, in all fitting procedures shown in Figs. 8 - 10 below, we take account the complete lattice range. We should note here that, recent Monte Carlo simulations of the model have been restricted to lattice sizes of the order of $L = 24$ [101]. The first set of our illustrations, Figs. 5 - 7, is rather instructive. We show various thermodynamic quantities for typical lattice sizes used in the scaling analysis below. In particular, in Fig. 5 we plot the specific heat of the model as a function of the temperature for three characteristic linear sizes, i.e., $L = 8, 16,$ and $L = 32$. One can observe from this figure the clear shift of the pseudocritical temperatures with increasing lattice size, as well as the increase in the value of the corresponding maximum. Figure 6 now shows for a lattice with linear size $L = 8$ the temperature behav-

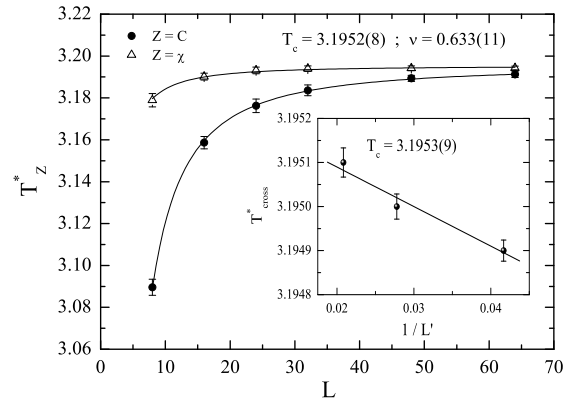


Fig. 8. Shift behavior of the pseudocritical temperatures of the specific heat and susceptibility for the 3d Blume-Capel model at the value $\Delta = 0$. The inset shows the FSS behavior of the crossings of the fourth-order Binder's cumulant with inverse lattice size (see also discussion in the text).

ior of the order parameter M in the main panel, and its corresponding deduced magnetic susceptibility χ in the inset. Finally, Fig. 7 shows the analogous L - dependence behavior of the susceptibility curves as a function of the temperature, where again, as in Fig. 5 the expected shift behavior is recovered.

We proceed now with the FSS analysis of our numerical data in Figs. 8 - 10. In particular, in the main panel of Fig. 8 we present the simultaneous fitting of two pseudocritical temperatures of the model, namely those of the specific heat C and magnetic susceptibility χ , according to the well-known power law $T_Z^* = T_c + b_Z L^{-1/\nu}$. The result we get for the critical temperature, also shown in the panel, $T_c = 3.1952(8)$, is in very good agreement with the Ornstein-Zernike approximation of the phase diagram of the model by Grollau *et al.* [103] and with the numerical estimation 3.20(1) given in Ref. [101]. Additionally, the estimated value of the critical exponent ν , $\nu = 0.633(11)$, is in excellent agreement with the value 0.6304(13) of the simple 3d Ising model [88] and the value 0.63002(10) quoted by the most accurate calculation of Hasenbusch for the second-order phase-transition regime of the Blume-Capel model [102]. This is a clear first strong indication of the Ising universality in the second-order regime of the Blume-Capel model. In the corresponding inset of Fig. 8 we illustrate a further test of our accuracy of the WL and BP approaches, by using the crossings of the fourth-order Binder's cumulant $U_L = 1 - \langle M^4 \rangle / [3\langle M^2 \rangle^2]$ [21]. We show three data points which denote the temperature crossing points (T_{cross}^*) of the Binder's cumulant for the following pairs of lattices: $(L_1, L_2) = (16, 32), (24, 48),$ and $(32, 64)$. The notation L' in the x-axis refers to the value $L' = (L_1 + L_2)/2$. The solid line is a simple linear fitting extrapolating to $L' \rightarrow \infty$, which gives an estimate for the critical temperature $T_c = 3.1953(9)$, also in very good agreement with the estimate of the main panel.

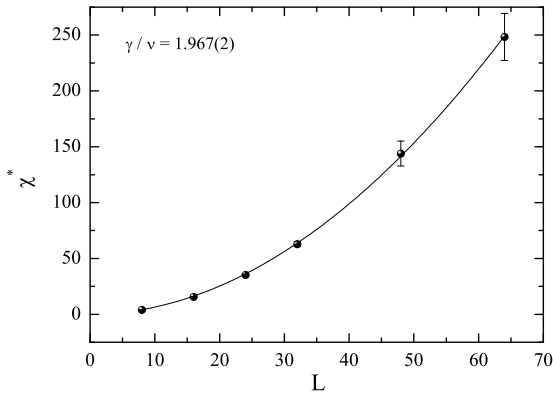


Fig. 9. FSS behavior of the magnetic susceptibility maxima of the 3d $\Delta = 0$ Blume-Capel model.

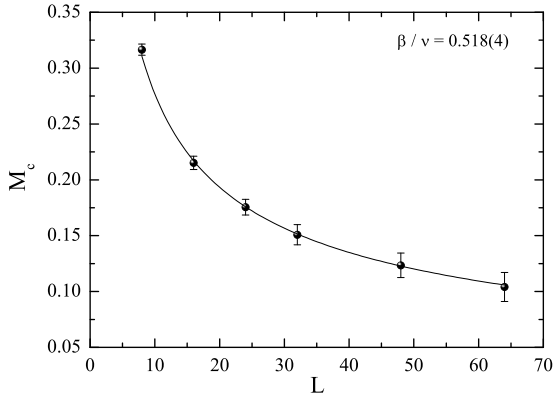


Fig. 10. FSS behavior of the critical order parameter data of the 3d $\Delta = 0$ Blume-Capel model.

We proceed with the estimation of the magnetic exponent ratios of the 3d Blume-Capel model at $\Delta = 0$. Figure 9 illustrates the FSS behavior of the magnetic susceptibility maxima which are expected to scale as $\chi^* \sim L^{\gamma/\nu}$ with the lattice size. The solid line is a fitting of the above form giving an estimate of 1.967(2) for the exponent ratio γ/ν , very close to the value 1.966(3) of the simple 3d Ising model [88]. In Fig. 10 we present numerical data for the order parameter M of the model at the estimated critical temperature of Fig. 8. The solid line is simple power-law fitting of the form $M_c \sim L^{-\beta/\nu}$ which gives the estimate 0.518(4) for the critical exponent ratio, very close to the value 0.517(3) of the corresponding pure Ising model [88]. We note here that, both of these magnetic exponent ratios are a considerable improvement of the recent numerical estimations of Özkan et al. [101] using two different procedures defined as the standard and cooling algorithms on a cellular automaton estimation that gave the values 1.94(4) and 0.48(6) for the exponent ratios γ/ν and β/ν , respectively.

Overall, the FSS analysis performed in this Section places, without doubt, the second-order phase-transition regime of Blume-Capel model to the universality class of the pure 3d Ising model. Additionally, the proposed estimates for the critical exponents clearly indicate the accuracy of the numerical scheme that is based on the WL algorithm.

4 Summary and outlook

Summarizing, in the present paper we reported large-scale numerical simulations of the random 2d Ising model and the pure 3d Blume-Capel model using a modified version of the Wang-Landau algorithm. For the first (random) model, both sets of the numerical data and the relevant finite-size scaling analysis for the two values of the disorder strength considered, clearly support the strong universality scenario hypothesis, through the estimated value of the correlation length's exponent $\nu \cong 1$. Furthermore, the accuracy of the simulation scheme via the Wang-Landau algorithm has been clearly shown via a direct comparison between the estimated values of the critical temperatures and the exact ones. For the latter (pure) model, our estimates of the critical exponents compare well with the most accurate ones in the current literature and place the second-order phase-transition regime of the Blume-Capel model to the universality class of the pure 3d Ising model, as also expected on theoretical grounds. Further attempts are currently being considered in order to obtain a complete numerical derivation of the Blume-Capel model's phase diagram by simulating several values of the crystal field Δ , including also those in the model's first-order phase-transition regime.

N.G.F. has been partly supported by MICINN, Spain, through Research Contract No. FIS2009-12648-C03. P.E.T. is grateful for financial support by the Austrian Science Foundation within the SFB ViCoM (Grant F41).

References

1. H.E. Stanley, Introduction to Phase Transitions and Critical Phenomena (Oxford U.P., Oxford, 1971)
2. K.G. Wilson, Phys. Rev. B **4**, 3174 (1971)
3. R.J. Baxter, Ann. Phys. **70**, 193 (1970)
4. J. Ashkin, E. Teller, Phys. Rev. **64**, 178 (1943).
5. J. Cardy, *Scaling and Renormalization in Statistical Physics*, (Cambridge University Press 1996)
6. A.P. Young (ed.), *Spin glasses and random fields*, (World Scientific, Singapore 1998)
7. M. Blume, Phys. Rev. **141**, 517 (1966)
8. H.W. Capel, Physica (Utr.) **32**, 966 (1966); H.W. Capel, Physica (Utr.) **33**, 295 (1967); H.W. Capel, Physica (Utr.) **37**, 423 (1967)
9. Vik.S. Dotsenko, Vl.S. Dotsenko, JETP Lett. **33**, 37 (1981)
10. G. Jug, Phys. Rev. B **27**, 4518 (1983)
11. B.N. Shalaev, Sov. Phys. Solid State **26**, 1811 (1984)
12. R. Shankar, Phys. Rev. Lett. **58**, 2466 (1987)

13. A.W.W. Ludwig, Nucl. Phys. B **285**, 97 (1987)
14. F. Wang, D.P. Landau, Phys. Rev. Lett. **86**, 2050 (2001); F. Wang, D.P. Landau, Phys. Rev. E **64**, 056101 (2001)
15. A. Malakis, A. Peratzakis, N.G. Fytas, Phys. Rev. E **70**, 066128 (2004); A. Malakis, S.S. Martinos, I.A. Hadjiagapiou, N.G. Fytas, P. Kalozoumis, Phys. Rev. E **72**, 066120 (2005)
16. R.E. Belardinelli, V.D. Pereyra, Phys. Rev. E **75**, 046701 (2007); R.E. Belardinelli, V.D. Pereyra, J. Chem. Phys. **127**, 184105 (2007)
17. N. Metropolis, A.W. Rosenbluth, M.N. Rosenbluth, A.H. Teller, J. Chem. Phys. **21**, 1087 (1953)
18. A.B. Bortz, M.H. Kalos, J.L. Lebowitz, J. Comput. Phys. **17**, 10 (1975)
19. K. Binder, Rep. Prog. Phys. **60**, 487 (1997)
20. M.E.J. Newman, G.T. Barkema, *Monte Carlo Methods in Statistical Physics* (Clarendon Press, Oxford, 1999)
21. D.P. Landau, K. Binder, *A Guide to Monte Carlo Simulations in Statistical Physics* (Cambridge University Press, Cambridge, 2000)
22. J. Lee, Phys. Rev. Lett. **71**, 211 (1993)
23. H.K. Lee, Y. Okabe, D.P. Landau, Comput. Phys. Commun. **175**, 36 (2006)
24. P.M.C. de Oliveira, T.J.P. Penna, H.J. Herrmann, Braz. J. Phys. **26**, 677 (1996)
25. J.-S. Wang, T.K. Tay, R.H. Swendsen, Phys. Rev. Lett. **82**, 476 (1999); J.-S. Wang, R.H. Swendsen, J. Stat. Phys. **106**, 245 (2002)
26. B.A. Berg, T. Neuhaus, Phys. Lett. B **276**, 249 (1991); B.A. Berg, T. Neuhaus, Phys. Rev. Lett. **68**, 9 (1992)
27. G.R. Smith, A.D. Bruce, J. Phys. A **28**, 6623 (1995)
28. G.M. Torrie, J.-P. Valleau, J. Comput. Phys. **23**, 187 (1997)
29. R.H. Swendsen, J.-S. Wang, Phys. Rev. Lett. **57**, 2607 (1986)
30. C.J. Geyer, *Computing Science and Statistics: Proceedings of the 23rd Symposium on the interface*, ed. E.K. Keramidas, Interface Foundation, Fairfax Station, New York, p. 156 (1991)
31. E. Marinari, G. Parisi, Europhys. Lett. **19**, 451 (1992)
32. A.P. Lyubartsev, A.A. Martynovskii, S.V. Shevkunov, P.N. Vorontsov-Velyaminov, J. Chem. Phys. **96**, 1776 (1992)
33. K. Hukushima, K. Nemoto, J. Phys. Soc. Jpn. **65**, 1604 (1996)
34. E. Marinari, G. Parisi, J.J. Ruiz-Lorenzo, *Spin Glasses and Random Fields*, ed. A.P. Young, Directions in Condensed Matter Physics, World Scientific, Singapore, Vol. 12 (1998)
35. S. Trebst, D.A. Huse, M. Troyer, Phys. Rev. E **70**, 046701 (2004)
36. N. Douarche, F. Calvo, G.M. Pastor, P.J. Jensen, Eur. Phys. J. D **24**, 77 (2003)
37. M. Troyer, S. Wessel, F. Alet, Phys. Rev. Lett. **90**, 120201 (2003)
38. A. Malakis, N.G. Fytas, Phys. Rev. E **73**, 056114 (2006); A. Malakis, N.G. Fytas, Phys. Rev. E **73**, 016109 (2006); N.G. Fytas, A. Malakis, Eur. Phys. J. B **61**, 111 (2008)
39. B.J. Schulz, K. Binder, M. Müller, Phys. Rev. E, **71**, 046705 (2005)
40. S. Reynal, H.T. Diep, Phys. Rev. E **72**, 056710 (2005)
41. D. Jayasri, V.S.S. Sastry, K.P.N. Murthy, Phys. Rev. E **72**, 036702 (2005)
42. S. Trebst, E. Gull, M. Troyer, J. Chem. Phys. **123**, 204501 (2005)
43. N. Rathore, J.J. de Pablo, J. Chem. Phys. **116**, 7225 (2002); N. Rathore, T.A. Knotts, J.J. de Pablo, J. Chem. Phys. **118**, 4285 (2003); N. Rathore, G. Yan, J.J. de Pablo, J. Chem. Phys. **120**, 5781 (2004); Q. Yan, R. Faller, J.J. de Pablo, J. Chem. Phys. **116**, 8745 (2002)
44. M.S. Shell, P.G. Debenedetti, A.Z. Panagiotopoulos, Phys. Rev. E **66**, 56703 (2002)
45. C. Yamaguchi, Y. Okabe, J. Phys. A **34**, 8781 (2001); Y. Okabe, Y. Tomita, C. Yamaguchi, Comput. Phys. Commun. **146**, 63 (2002)
46. V. Varshney, G.A. Carri, Phys. Rev. Lett. **95**, 168304 (2005); G.A. Carri, R. Batman, V. Varshney, T.E. Dirama, Polymer **46**, 3809 (2006)
47. F. Calvo, Mol. Phys. **100**, 3421 (2002); F. Calvo, P. Parneix, J. Chem. Phys. **119**, 256 (2003)
48. S.-H. Tsai, F. Wang, D.P. Landau, Phys. Rev. E **75**, 061108 (2007); Braz. J. Phys. **38**, 6 (2008); D.T. Seaton, S.J. Mitchell, D.P. Landau, Braz. J. Phys. **38**, 48 (2008); S.J. Mitchell, F.C. Luiz Pereira, D.P. Landau, Braz. J. Phys. **38**, 1 (2008)
49. P.N. Vorontsov-Velyaminov, N.A. Volkov, A. Yurchenko, J. Phys. A **37**, 1573 (2004); N.A. Volkov, P.N. Vorontsov-Velyaminov, A.P. Lyubartsev, Phys. Rev. E **75**, 016705 (2007)
50. P. Poulain, F. Calvo, R. Antoine, M. Broyer, P. Dugourd, Phys. Rev. E **73**, 056704 (2006)
51. B.J. Schulz, K. Binder, M. Müller, D.P. Landau, Phys. Rev. E **67**, 067102 (2003)
52. P. Dayal, S. Trebst, S. Wessel, D. Würtz, M. Troyer, S. Sabhapandit, S.N. Coppersmith, Phys. Rev. Lett. **92**, 097201 (2004)
53. N.G. Fytas, A. Malakis, K. Eftaxias, J. Stat. Mech.: Theory Exp. (2008) P03015; A. Malakis, A.N. Berker, I.A. Hadjiagapiou, N.G. Fytas, Phys. Rev. E **79**, 011125 (2009); N.G. Fytas, A. Malakis, Phys. Rev. E **81**, 041109 (2010)
54. S. Alder, S. Trebst, A.K. Hartmann, M. Troyer, J. Stat. Mech.: Theory Exp. (2004) P07008
55. C. Zhou, R.N. Bhatt, Phys. Rev. E **72**, 025701(R) (2005); C. Zhou, T.C. Schulthess, S. Torbrügge, D.P. Landau, Phys. Rev. Lett. **96**, 120201 (2006)
56. D.F. Parsons, D.R.M. Williams, Phys. Rev. E **74**, 041804 (2006); D.F. Parsons, D.R.M. Williams, J. Chem. Phys. **124**, 221103 (2006)
57. A.G. Cunha Netto, C.J. Silva, A.A. Caparica, R. Dickman, Braz. J. Phys. **36**, 619 (2006)
58. D. Antypov, J.A. Elliott, Macromolecules **41**, 7243 (2008)
59. T. Wüst, D.P. Landau, Comp. Phys. Commun. **179**, 124 (2008)
60. D.T. Seaton, T. Wüst, D.P. Landau, Comp. Phys. Commun. **180**, 587 (2009); D.T. Seaton, T. Wüst, D.P. Landau, Phys. Rev. E **81**, 011802 (2010)
61. M.P. Taylor, W. Paul, K. Binder, Phys. Rev. E **79**, 050801(R) (2009); M.P. Taylor, W. Paul, K. Binder, J. Chem. Phys. **131**, 114907 (2009)
62. N.G. Fytas, P.E. Theodorakis, Phys. Rev. E **82**, 06201 (2010); P.E. Theodorakis, N.G. Fytas, Eur. Phys. J. B **81**, 245 (2011)
63. Z. Wang, X. He, J. Chem. Phys. **135**, 094902 (2011)
64. M. Aizenman, J. Wehr, Phys. Rev. Lett. **62**, 2503 (1989); M. Aizenman, J. Wehr, Phys. Rev. Lett. **64**, 1311(E) (1990)
65. K. Hui, A.N. Berker, Phys. Rev. Lett. **62**, 2507 (1989); K. Hui, A.N. Berker, Phys. Rev. Lett. **63**, 2433(E) (1989)
66. A.N. Berker, Physica A **194**, 72 (1993)

67. S. Chen, A.M. Ferrenberg, D.P. Landau, Phys. Rev. Lett. **69**, 1213 (1992); S. Chen, A.M. Ferrenberg, D.P. Landau, Phys. Rev. E **52**, 1377 (1995)
68. J. Cardy, J. Phys. A **29**, 1897 (1996)
69. J. Cardy, J.L. Jacobsen, Phys. Rev. Lett. **79**, 4063 (1997)
70. C. Chatelain, B. Berche, Phys. Rev. Lett. **80**, 1670 (1998)
71. R. Paredes V., J. Valbuena, Phys. Rev. E **59**, 6275 (1999)
72. C. Chatelain, B. Berche, W. Janke, P.E. Berche, Phys. Rev. E **64**, 036120 (2001)
73. L.A. Fernández, A. Gordillo-Guerrero, V. Martín-Mayor, J.J. Ruiz-Lorenzo, Phys. Rev. Lett. **100**, 057201 (2008)
74. A.B. Harris, J. Phys. C **7**, 1671 (1974)
75. J.T. Chayes, L. Chayes, D.S. Fisher, T. Spencer, Phys. Rev. Lett. **57**, 2999 (1986)
76. V. Dotsenko, M. Picco, P. Pujol, Nucl. Phys. B **455**, 701 (1995)
77. J.L. Jacobsen, J. Cardy, Nucl. Phys. B **515**, 701 (1998)
78. G. Mazzeo, R. Kühn, Phys. Rev. E **60**, 3823 (1999)
79. R. Kenna, D.A. Johnston, W. Janke, Phys. Rev. Lett. **96**, 115701 (2006); R. Kenna, D.A. Johnston, W. Janke, Phys. Rev. Lett. **97**, 155702 (2006)
80. A. Gordillo-Guerrero, R. Kenna, J.J. Ruiz Lorenzo, AIP Conf. Proc. **1198**, 42 (2009)
81. J.-S. Wang, W. Selke, V.I.S. Dotsenko, V.B. Andreichenko, Physica A **164**, 221 (1990)
82. J.-K. Kim, A. Patrascioiu, Phys. Rev. Lett. **72**, 2785 (1994); J.-K. Kim, A. Patrascioiu, Phys. Rev. B **49**, 15764 (1994); W. Selke, Phys. Rev. Lett. **73**, 3487 (1994); K. Ziegler, Phys. Rev. Lett. **73**, 3488 (1994); J.-K. Kim, A. Patrascioiu, Phys. Rev. Lett. **73**, 3489 (1994); J.-K. Kim, Phys. Rev. B **61**, 1246 (2000)
83. R. Kühn, Phys. Rev. Lett. **73**, 2268 (1994)
84. M. Suzuki, Prog. Theor. Phys. **51**, 1992 (1974)
85. J.D. Gunton, T. Niemeijer, Phys. Rev. B **11**, 567 (1975)
86. R. Fisch, J. Stat. Phys. **18**, 111 (1978)
87. A. Malakis, A.N. Berker, I.A. Hadjiagapiou, N.G. Fytas, Phys. Rev. E **79**, 011125 (2009); A. Malakis, A.N. Berker, I.A. Hadjiagapiou, N.G. Fytas, T. Papakonstantinou, Phys. Rev. E **81**, 041113 (2010)
88. R. Guida, J. Zimm-Justin, J. Phys. A **31**, 8103 (1998)
89. A. Pelissetto, E. Vicari, Phys. Rep. **368**, 549 (2002)
90. D.P. Landau, Phys. Rev. Lett. **28**, 449 (1972); A.N. Berker, M. Wortis, Phys. Rev. B **14**, 4946 (1976); M. Kaufman, R.B. Griffiths, J.M. Yeomans, M. Fisher, Phys. Rev. B **23**, 3448 (1981); W. Selke, J. Yeomans, J. Phys. A **16**, 2789 (1983); D.P. Landau, R.H. Swendsen, Phys. Rev. B **33**, 7700 (1986); J.C. Xavier, F.C. Alcaraz, D. Pena Lara, J.A. Plascak, Phys. Rev. B **57**, 11575 (1998)
91. M.J. Stephen, J.L. McCole, Phys. Rev. Lett. **44**, 89 (1973); T.S. Chang, G.F. Tuthill, H.E. Stanley, Phys. Rev. B **9**, 4482 (1974); G.F. Tuthill, J.F. Nicoll, H.E. Stanley, Phys. Rev. B **11**, 4579 (1975); F.J. Wegner, Phys. Lett. **54A**, 1 (1975)
92. P.F. Fox, A.J. Guttmann, J. Phys. C **6**, 913 (1973); T.W. Burkhardt, R.H. Swendsen, Phys. Rev. B **13**, 3071 (1976); W.J. Camp, J.P. Van Dyke, Phys. Rev. B **11**, 2579 (1975); D.M. Saul, M. Wortis, D. Stauffer, Phys. Rev. B **9**, 4964 (1974)
93. P. Nightingale, J. Appl. Phys. **53**, 7927 (1982)
94. P.D. Beale, Phys. Rev. B **33**, 1717 (1986)
95. A.K. Jain, D.P. Landau, Phys. Rev. B **22**, 445 (1980)
96. D.P. Landau, R.H. Swendsen, Phys. Rev. Lett. **46**, 1437 (1981)
97. C.M. Care, J. Phys. A **26**, 1481 (1993)
98. M. Deserno, Phys. Rev. E **56**, 5204 (1997)
99. Y. Deng, H.W.J. Blöte, Phys. Rev. E **68**, 036125 (2003)
100. C.J. Silva, A.A. Caparica, J.A. Plascak, Phys. Rev. E **73**, 036702 (2006)
101. A. Özkan, N. Seferoğlu, B. Kutlu, Physica A **362**, 327 (2005)
102. M. Hasenbusch, Phys. Rev. B **82**, 174433 (2010)
103. S. Grollau, E. Kierlik, M.L. Rosinberg, G. Tarjus, Phys. Rev. E **63**, 041111 (2001)